

# Many-body T-matrix of a two-dimensional Bose-Einstein condensate within the Hartree-Fock-Bogoliubov formalism

Christopher Gies<sup>†</sup>, MD Lee<sup>‡</sup> and DAW Hutchinson<sup>†</sup>

E-mail: cluso@physics.otago.ac.nz, m.lee1@physics.ox.ac.uk,  
hutch@physics.otago.ac.nz

<sup>†</sup>Department of Physics, University of Otago, P.O. Box 56, Dunedin, New Zealand

<sup>‡</sup>Clarendon Laboratory, Department of Physics, University of Oxford, Parks Road, Oxford OX1 3PU, United Kingdom

**Abstract.** In a two-dimensional Bose-Einstein condensate the reduction in dimensionality fundamentally influences collisions between the atoms. In the crossover regime from three to two dimensions several scattering parameters have been considered. However, finite temperature results are more difficult to obtain. In this work we present the many-body T-matrix at finite temperatures within a gapless Hartree-Fock-Bogoliubov approach and compare to zero and finite temperature results obtained using different approaches. A semi-classical renormalization method is used to remove the ultra-violet divergence of the anomalous average.

PACS numbers: 03.65.Nk, 03.75.Hh, 03.75.Nt, 05.30.Jp

Submitted to: *J. Phys. B: At. Mol. Phys.*

## 1. Introduction

When interaction processes within a Bose-condensed gas of atoms are considered, collisions are often characterized by the two-body transition matrix (T-matrix), evaluated in the limit of zero energy and collision momenta. In three dimensions, this leads to the well-known expression  $g = 4\pi\hbar^2 a_{3D}/m$  for the coupling parameter, with  $a_{3D}$  being the three-dimensional, measured,  $s$ -wave scattering length and  $m$  the mass of the atoms. The two-body T-matrix incorporates only binary collisions and neglects effects that are due to the surrounding atoms. In three dimensions these many-body effects have been shown to become important only in the regime close to the critical temperature and are normally neglected (Hutchinson et al. 1998). In a two-dimensional system, however, scattering processes are influenced by the reduction in dimensionality and the two-body T-matrix differs from that in the three-dimensional case (Stoof & Bijlsma 1993, Bijlsma & Stoof 1997, Petrov et al. 2000, Petrov & Shlyapnikov 2001). In the literature various approaches have been invoked in order to obtain a valid coupling parameter for a Bose-Einstein condensate (BEC) in the two-dimensional regime. If many-body effects are neglected, the interaction strength

has been shown to exhibit a logarithmic dependence on the collision energy (Schick 1971, Fischer & Hohenberg 1988, Stoof et al. 1988, Kolomeisky & Straley 1992, Stoof & Bijlsma 1993, Bijlsma & Stoof 1997, Kolomeisky et al. 2000, Morgan et al. 2002) which goes to zero in the limit of zero collision energy. Therefore, in the description of condensates, many-body effects dominate even in the first order approximation, and so the determination of a many-body T-matrix which includes these effects is of fundamental importance when studying two-dimensional BECs.

The Hartree-Fock-Bogoliubov (HFB) theory has proven successful in describing finite temperature properties of dilute Bose gases (Hutchinson et al. 1997, Hutchinson et al. 2000, Hutchinson & Morgan 2002). Many-body effects on scattering processes are included in the theory through the anomalous pair average. However, the full HFB theory is known to contain various inconsistencies, such as a gap in the excitation spectrum and ultra-violet divergences. To render the theory consistent, gapless extensions have been developed (Proukakis et al. 1998, Hutchinson et al. 1998, Hutchinson et al. 2000). In this work, we use the gapless HFB theory, together with a semi-classical renormalization procedure to remove the ultra-violet divergence of the anomalous average, to study many-body effects on interactions. Many-body effects due to the anomalous pair average can be neglected by taking the simpler Popov approximation, which we have previously used to investigate the failure of the semi-classical approximation in two dimensions (Gies et al. 2004) and to study the coherence properties of the two-dimensional BEC (Gies & Hutchinson 2004). However, the problem of zero interaction strength in the two-body limit of the coupling parameter persists and an appropriate effective contact interaction strength has to be used.

Lee *et al* have shown that, at zero temperature, the many-body T-matrix can be expressed in terms of the two-body T-matrix, evaluated at a shifted off-shell energy (Lee et al. 2002). Recently, this approach has been extended to finite temperatures by Rajagopal *et al* for a homogeneous system (Rajagopal et al. 2004). We compare results from both these approaches at zero and finite temperatures to the results obtained from the gapless HFB method, using local density approximations to incorporate the spatial dependence of the condensate density in the trap.

The underlying theory is outlined in the following section. We briefly summarize the gapless HFB method and how it incorporates many-body effects before discussing in detail the renormalization of the anomalous average in Section 2.1.1. In Sections 2.2 and 2.2.3 we outline the meaning of the many-body T-matrix and how it can be expressed in terms of two-body coupling parameters, depending on the regime in the dimensional crossover from three to two dimensions, both at zero and finite temperatures. In Section 3 we then present our numerical results for the renormalized anomalous average and the many-body T-matrix.

## 2. Theory

### 2.1. Gapless Hartree-Fock-Bogoliubov formalism

Within the HFB formalism the static properties of the BEC are described by a coupled set of equations that require a self-consistent solution (Hutchinson et al. 2000, Griffin 1996). The order parameter  $\Psi_0(\mathbf{r})$  which describes the condensed phase, obeys a generalized Gross-Pitaevskii equation (GPE)

$$\left( \hat{h}(\mathbf{r}) - \mu + g_{\text{con}}(\mathbf{r}) n_c(\mathbf{r}) + 2g_{\text{exc}}(\mathbf{r}) \tilde{n}(\mathbf{r}) \right) \Psi_0(\mathbf{r}) = 0, \quad (1)$$

while the thermal cloud is determined by the quasiparticle amplitudes,  $u_i, v_i$ , and quasiparticle energies,  $E_i$ , which obey the coupled Bogoliubov-de Gennes (BdG) equations

$$\begin{aligned}\hat{\mathcal{L}} u_i(\mathbf{r}) - \mathcal{M} v_i(\mathbf{r}) &= E_i u_i(\mathbf{r}) \\ \hat{\mathcal{L}} v_i(\mathbf{r}) - \mathcal{M} u_i(\mathbf{r}) &= -E_i v_i(\mathbf{r}) .\end{aligned}\quad (2)$$

Here

$$\hat{\mathcal{L}} = \hat{h}(\mathbf{r}) - \mu + 2 \left( g_{\text{con}}(\mathbf{r}) n_c(\mathbf{r}) + g_{\text{exc}}(\mathbf{r}) \tilde{n}(\mathbf{r}) \right), \quad (3)$$

and,

$$\mathcal{M} = g_{\text{con}}(\mathbf{r}) n_c(\mathbf{r}) . \quad (4)$$

$\hat{h}(\mathbf{r}) = -\hbar^2 \Delta / 2m + U_{\text{trap}}$  is the single particle Hamiltonian, and  $n_c(\mathbf{r})$ ,  $\tilde{n}(\mathbf{r})$  and  $n(\mathbf{r}) = n_c(\mathbf{r}) + \tilde{n}(\mathbf{r})$  refer to the condensate, non-condensate and total densities respectively. In (1) and (2) we have written the HFB equations in a generalized form which, as we point out, is not precisely the full HFB theory as derived in (Griffin 1996). It has been shown that the occurrence of the anomalous pair average  $\tilde{m}(\mathbf{r}) = \langle \delta \hat{\psi}(\mathbf{r}) \delta \hat{\psi}(\mathbf{r}) \rangle$  leads to a gap in the excitation spectrum (Griffin 1996). This, however, is forbidden by Goldstone's theorem (Goldstone 1961) or the more general Hugenholtz-Pines theorem (Hugenholtz & Pines 1959). Several resolutions to this problem exist. One can neglect the anomalous average completely; the so-called Popov approximation. However, the anomalous average has been shown to introduce many-body effects via the many-body T-matrix for scattering processes (Proukakis et al. 1998, Morgan 2000) through

$$T_{\text{mb}}^{\text{GHFB}}(\mathbf{r}) = g \left( 1 + \frac{\tilde{m}(\mathbf{r})}{\Psi_0(\mathbf{r})^2} \right) . \quad (5)$$

Thus, the Popov approximation neglects these many-body effects. The problems from which the full HFB theory suffers stem from the inconsistent introduction of these effects. Gapless extensions to the full HFB theory have been developed that do not neglect the anomalous average, but rather render the theory consistent by making sure these effects are accounted for equally for all classes of scattering processes. These theories have been termed G1 and G2 and can be identified by the definition of the coupling parameters in (1) and (2) (Proukakis et al. 1998, Hutchinson et al. 2000), i. e.

$$g_{\text{con}}(\mathbf{r}) = T_{\text{mb}}^{\text{GHFB}}(\mathbf{r}), \quad g_{\text{exc}} = g \quad \text{for G1} \quad (6)$$

$$g_{\text{con}}(\mathbf{r}) = T_{\text{mb}}^{\text{GHFB}}(\mathbf{r}), \quad g_{\text{exc}}(\mathbf{r}) = T_{\text{mb}}^{\text{GHFB}}(\mathbf{r}) \quad \text{for G2} . \quad (7)$$

The G1 theory includes many-body effects only for collisions within the condensate and has been shown to be justified by a perturbative second order treatment of the full HFB theory (Morgan 2000). The G2 extension also includes many-body effects for condensate–non-condensate interactions, and has been applied successfully to explain the downward shift in the  $m = 2$  excitation frequency for an anisotropically trapped three-dimensional BEC (Hutchinson et al. 1998) at temperatures approaching the critical temperature. Note that equation (5) requires the knowledge of the coupling parameter  $g$  in the two-body limit. We discuss the determination of  $g$  in Section 2.2.2.

Both the non-condensate density and the anomalous average are calculated by populating the quasiparticle levels via the Bose distribution function:

$$\tilde{n}(\mathbf{r}) = \sum_i f_B(E_i) \left( |u_i(\mathbf{r})|^2 + |v_i(\mathbf{r})|^2 \right) + |v_i(\mathbf{r})|^2 \quad (8)$$

$$\tilde{m}(\mathbf{r}) = \sum_i \left( 2f_B(E_i) + 1 \right) u_i(\mathbf{r})v_i^*(\mathbf{r}) . \quad (9)$$

The Bose distribution function with the inverse temperature  $\beta = 1/k_B T$  is given by  $f_B(E_i) = [z^{-1}e^{\beta E_i} - 1]^{-1}$  with the fugacity  $z^{-1} = 1 + N_0^{-1}$ .

While the summations in (8) and (9) are infinite, when calculating numerical solutions to this system of equations, we are compelled to introduce a high energy cut-off  $\epsilon_{\text{cut}}$ . We use a semi-classical treatment (Reidl et al. 1999, Gies & Hutchinson 2004) to calculate the contributions to  $\tilde{n}$  and  $\tilde{m}$  from above the cut-off, and also to perform a necessary renormalization of the anomalous average, as discussed in the following section.

*2.1.1. Renormalization of the anomalous average.* To go beyond the Popov approximation, the many-body T-matrix must be calculated from (5). In order to obtain a divergence free anomalous average, the vacuum contributions already included in the measured value of the  $s$ -wave scattering length must be explicitly subtracted. To motivate the renormalization procedure, we briefly discuss its origin through the relation between the anomalous average and the many-body T-matrix. In the homogeneous limit the off-diagonal matrix element  $\mathcal{M}$  (4), which is defined in terms of the bare interaction potential  $V(\mathbf{r} - \mathbf{r}')$ , obeys a Lippmann-Schwinger equation and can be identified with the many-body T-matrix. In the pseudo potential approximation (Huang 1987), the matrix elements of the bare interaction potential are replaced by the contact interaction  $\delta$ -potential, which leads to ultra-violet divergences in the gapless HFB theories. In fact, the contact potential approximation is better applied to the two-body T-matrix. Introducing the two-body T-matrix and taking the contact potential approximations leads to the inclusion of an additional term which, together with  $\tilde{m}$ , we identify as a renormalized anomalous average  $\tilde{m}^R$ . Replacing the bare interaction potential by the two-body T-matrix is consistent to all orders in the Lippmann-Schwinger equation which defines the many-body T-matrix if it is accompanied by this renormalization (Proukakis et al. 1998, Morgan 2000). The equations which give the gapless HFB theories are unchanged, save for the replacement of the anomalous average by  $\tilde{m}^R$  everywhere that it appears.

We now describe how we obtain the divergence free anomalous average. To simplify the formulation within this section, we omit the notation of spatial dependencies and introduce the following notation for the different parts of the anomalous average

$$\begin{aligned} \tilde{m}^R &= \sum_i^{E_i < \epsilon_{\text{cut}}} (2f_B(E_i) + 1) u_i v_i \\ &\quad + \int_{\epsilon_{\text{cut}}}^{\infty} dE \{ \tilde{m}'_{\text{sc}}(E) - \tilde{m}'_{\text{r}}(E) \} - \int_0^{\epsilon_{\text{cut}}} dE \tilde{m}'_{\text{r}}(E) \\ &\equiv \tilde{m}_{\text{qm}} + \tilde{m}_1 - \tilde{m}_2 . \end{aligned} \quad (10)$$

Here, the first part  $\tilde{m}_{\text{qm}}$  is calculated quantum mechanically by explicitly evaluating the sum in (9) up to the energy cutoff. The second part,  $\tilde{m}_1$ , contains the contribution

from the energy levels above the cutoff  $\epsilon_{\text{cut}}$ , given by subtracting the renormalization term  $\tilde{m}'_r$  from the semiclassical anomalous average integrand  $\tilde{m}'_{\text{sc}}$ . The third part,  $\tilde{m}_2$ , is the renormalization of  $\tilde{m}_{\text{qm}}$ . Both  $\tilde{m}_1$  and  $\tilde{m}_2$  are calculated within the semi-classical approximation.

In analogy to the semi-classical expression for the non-condensate density in two dimensions, see (Gies & Hutchinson 2004), the unrenormalized semi-classical expression for the anomalous average integrand can be found to be

$$\begin{aligned} \tilde{m}'_{\text{sc}}(E) = & -\frac{m}{2\pi\hbar^2} (2f_{\text{B}}(E) + 1) \frac{gn_c}{\sqrt{E^2 + (gn_c)^2}} \\ & \times \Theta \left( E - \sqrt{(U_{\text{trap}} - \mu + 2gn)^2 - (gn_c)^2} \right). \end{aligned} \quad (11)$$

The integral is logarithmically divergent for the non-thermal part on the upper boundary, but this divergence is removed by the renormalization. To calculate the excessive contribution to the anomalous average, we consider the case  $n_c \rightarrow 0$ . In this sense we keep only terms linear in the condensate density. This arises from the assumption that we renormalize the vacuum contributions to  $\tilde{m}$  at zero temperature that have already been accounted for in the measured scattering length in the two-body T-matrix. In the limit that there is no condensate present, the quasiparticle energies are replaced by the single particle energies. Since the quasiparticle energies are measured relative to the condensate, we replace

$$E \rightarrow E + \mu. \quad (12)$$

Doing so in (11) and regarding only the temperature independent part leads to

$$\tilde{m}'_r(E) = -\frac{m}{2\pi\hbar^2} \frac{gn_c}{E + \mu}. \quad (13)$$

*Above the Energy Cutoff.* We can now calculate the semi-classical contribution to  $\tilde{m}^R$  from above the energy cutoff, i. e.

$$\tilde{m}_1 = \int_{E_{\text{min}}}^{\infty} dE (\tilde{m}'_{\text{sc}}(E) - \tilde{m}'_r(E)). \quad (14)$$

The lower limit of the integral is determined by the maximum of the Heaviside function in (11) and the cutoff energy, i. e.

$$E_{\text{min}} = \max \left\{ \epsilon_{\text{cut}}, \sqrt{(U_{\text{trap}} - \mu + 2gn)^2 - (gn_c)^2} \right\}. \quad (15)$$

Note that the shift of the energy in the denominator of (13) prevents the integral from being singular at the upper limit.

Since the semi-classical part (11) of the anomalous average is divergent at the upper boundary, the renormalization (13) must be subtracted under the same integral, so that we get for (14)

$$\tilde{m}_1 = -\frac{m}{2\pi\hbar^2} \int_{E_{\text{min}}}^{\infty} dE gn_c \left( \frac{2f_{\text{B}}(E) + 1}{\sqrt{E^2 - (gn_c)^2}} - \frac{1}{E + \mu} \right). \quad (16)$$

*Below the Energy Cutoff.* Since the sum in  $\tilde{m}_{\text{qm}}$  has a natural cutoff it does not diverge in the calculation. However, it contains contributions from the zero-temperature limit that must be renormalized by subtracting the integral of  $\tilde{m}'_i$  below the energy cutoff. In analogy to (13), this is given by

$$\tilde{m}_2 = -\frac{m}{2\pi\hbar^2} \int_0^{E_{\text{min}}} dE \frac{gn_c}{E + \mu} . \quad (17)$$

## 2.2. Determination of the many-body T-matrix

In three dimensions the effect of the surrounding medium on the scattering of two atoms plays a role only at high temperatures (Hutchinson et al. 1998). However, in the lower dimensional case these effects must be accounted for even at zero temperature, leading to the introduction of the many-body T-matrix (Bijlsma & Stoof 1997, Proukakis et al. 1998, Lee et al. 2002).

The many-body T-matrix used here is defined by the Lippmann-Schwinger equation

$$\begin{aligned} \langle \mathbf{k}' | T_{\text{mb}}(E) | \mathbf{k} \rangle &= \langle \mathbf{k}' | V(\mathbf{r}) | \mathbf{k} \rangle \\ &+ \sum_{\mathbf{q}} \langle \mathbf{k}' | V(\mathbf{r}) | \mathbf{q} \rangle \frac{1 + n_{\mathbf{q}} + n_{-\mathbf{q}}}{E - (E_{\mathbf{q}} + E_{-\mathbf{q}})} \langle \mathbf{q} | T_{\text{mb}}(E) | \mathbf{k} \rangle . \end{aligned} \quad (18)$$

This differs from the two-body T-matrix by the use of the quasiparticle energy spectrum for the intermediate states in a collision, and by the Bose enhancement of scattering into these states, given by the population terms. In the case of BEC, usually the zero momentum and energy limit is considered.

In the previous section we have briefly mentioned that the many-body T-matrix can be calculated by means of the anomalous average and the condensate wave function. Lee *et al* (Lee et al. 2002) have shown that in two dimensions, at zero temperature, the many-body T-matrix can be obtained from the known expression for the two-body T-matrix at an off-shell shifted collision energy, i. e.

$$T_{\text{mb}} = T_{2\text{b}}(-\mu) . \quad (19)$$

This result includes the effect of the quasiparticle energy spectrum of the intermediate states in the collision and provides a convenient method of calculating the many-body T-matrix. This should not be confused with the approach recently used by other authors (Khawaja et al. 2002, Rajagopal et al. 2004, Stoof & Bijlsma 1993), who have also used a shifted energy in the two-body T-matrix, namely an energy of  $-2\mu$ . The latter result stems from the argument that the excitation of a single condensate atom is associated with an energy of  $-\mu$ , so that for a condensate–condensate interaction the energy of the collision is then  $-2\mu$ . Such an argument includes only the mean-field energy of the initial and final states, and neglects the other many-body effects on the collision which are included in the result in (19).

The off-shell two-body T-matrix has been calculated for the genuinely two-dimensional case (Morgan et al. 2002), and using (19) we can obtain the many-body T-matrix. Experimental realizations of a two-dimensional system are not genuinely two-dimensional however, and different regimes in the dimensional crossover must be distinguished, which we now discuss.

*2.2.1. Two-body coupling parameter.* Interactions in a three-dimensional condensate are usually parameterized by the three dimensional coupling parameter  $g_{3D} = 4\pi\hbar^2 a_{3D}/m$ , which is the zero-temperature and zero-energy limit of the two-body T-matrix in three dimensions.

As the axial confinement of the trap is tightened, so that the dynamics of the atoms in the axial direction are frozen out, the dimension of the condensate is reduced from three to two dimensions. However, since scattering processes take place on a very small length scale, they can still be considered to take place in three spatial dimensions as long as the three dimensional scattering length  $a_{3D}$  is much smaller than the characteristic length of the trap,  $l_z = \sqrt{\hbar/m\omega_z}$ , with  $\omega_z$  the axial trapping frequency. During this crossover, the system can be classified into three different regimes: quasi-3D, quasi-2D and genuine 2D, where the latter, in which scattering itself is purely two-dimensional, is as yet inaccessible to experiment.

In the quasi-3D regime where  $l_z \gg a_{3D}$ , the axial  $z$ -component of the condensate wave function can be assumed to be Gaussian. Scattering is not directly affected by the axial confinement, and the tightly confined part can be factorized from the wave function, leading to a two-dimensional GPE with a modified interaction strength (Lee et al. 2002), i. e.

$$g_{q3D} = \sqrt{\frac{m\omega_z}{2\pi\hbar}} g_{3D}. \quad (20)$$

If the axial confinement is tightened further, collisions are influenced by the reduced dimensionality and the scattering problem must be considered explicitly. The quasi-2D regime, where  $l_z \gtrsim a_{3D}$ , has previously been investigated by Petrov *et al* (Petrov & Shlyapnikov 2001, Petrov et al. 2000). They found that the coupling parameter depends logarithmically on the tightness of the confinement and the collision energy. This regime is currently accessible to experiments (Görlitz et al. 2001) and forms the case we consider in the remainder of this paper. In order to obtain the many-body T-matrix, we evaluate the two-body coupling parameter at the negative energy  $-\mu$  corresponding to (19). For the homogeneous gas this can be written as (Lee et al. 2002)

$$g_{q2D} \equiv T_{\text{mb}}(E = 0) = \frac{4\pi\hbar^2}{m} \frac{1}{\ln(4\hbar^2/\mu m a_{2D}^2)}, \quad (21)$$

where the two-dimensional scattering length is given in terms of the three dimensional scattering length and the parameter  $l_z/a_{3D}$  by

$$a_{2D} = 4 \sqrt{\frac{\pi}{B}} l_z e^{-\sqrt{\pi} \frac{l_z}{a_{3D}}}, \quad (22)$$

with the constant  $B \approx 0.915$ . Note that (21) is valid strictly only at zero temperature. Because this form of the many-body T-matrix is valid in the quasi-2D regime, we refer to (21) with (22) as the *quasi-2D coupling parameter*.

In the genuine two-dimensional limit, where  $l_z \lesssim a_{3D}$ , the scattering length  $a_{2D}$  in (21) is a purely two dimensional quantity and cannot be approximated by (22). Since this regime is currently not experimentally accessible, we do not discuss details, but refer to (Tanatar et al. 2002, Lee et al. 2002).

The expressions given above are strictly valid only for a gas which is homogeneous in the two relevant dimensions. Provided that the trapping potential varies slowly on the length scale on which interactions take place, we can use the zero-temperature

relation  $\mu = gn_c(\mathbf{r})$  to replace the chemical potential within a local density approximation. This results in the spatially dependent coupling parameter in the quasi-2D regime

$$g_{\text{q2D}}(\mathbf{r}) = \frac{4\pi\hbar^2}{m} \frac{1}{\ln(4\hbar^2/n_c(\mathbf{r})g_{\text{q2D}}(\mathbf{r})ma_{2\text{D}}^2)} \quad (23)$$

which can be crudely approximated by

$$g_{\text{q2D}}(\mathbf{r}) \approx -\frac{4\pi\hbar^2}{m} \frac{1}{\ln(n_c(\mathbf{r})\pi a_{2\text{D}}^2)}. \quad (24)$$

This approximation overestimates (23), but we use it as a starting value in our first iteration to solve (23) self-consistently.

*2.2.2. Coupling strength  $g$  in gapless HFB.* The interaction strength  $g$  in (5) is defined by the two-body coupling parameter. In two dimensions this is given by (21) in the limit  $\mu = E = 0$  and hence vanishes, thus the determination of  $g$  is not straightforward. Naturally, since the many-body T-matrix from the gapless HFB approach must agree with the quasi-2D coupling parameter from the previous section, we can use this to determine the interaction strength  $g$ . Equations (21) and (23) are valid at zero temperature, and we solve the HFB equations self-consistently at zero temperature to determine  $g$  so that the gapless HFB many-body T-matrix agrees with the quasi-2D coupling parameter (23) at the trap centre.

*2.2.3. Extension to finite temperatures* The quasi-2D coupling parameter given in Section 2.2.1 was derived using the zero temperature relationship of (19). As a consequence, the effect of the population terms in (18) have been neglected. At finite temperatures these population terms will become significant and an extension to the results of Section 2.2.1 is required. Such an extension presents a significant problem. In the approach outlined in Section 2.2.1 the many-body T-matrix was calculated first in a homogeneous 2D zero-temperature system, before using the local density approximation to extend the results to the trapped case. At finite temperatures, however, a condensate cannot exist in a 2D homogeneous system. As a consequence, the calculation of the homogeneous finite temperature many-body T-matrix is plagued by infra-red divergences. In principle, the correct procedure would require the solution of the many-body scattering problem in a trap, but this is extremely difficult. A potential extension which avoids the problem of divergences was proposed in a recent publication by Rajagopal *et al* (Rajagopal *et al.* 2004). In their work the quasiparticle spectrum is approximated by  $E_i \approx E_i^{sp} + \mu$  (where  $E_i^{sp}$  is the single-particle energy spectrum), which is valid for the high energy states, but which neglects the phonon part of the spectrum. Using this approximation, the finite temperature result for the coupling parameter of Rajagopal *et al* is given by

$$g_{\text{q2D}}(T) = \frac{4\pi\hbar^2}{m} \frac{1}{\ln\left(\frac{4\hbar^2}{\mu a_{2\text{D}}^2}\right) - 2\sum_{s=1}^{\infty} \text{Ei}\left(\frac{-s\mu}{k_{\text{B}}T}\right)}. \quad (25)$$

where  $\text{Ei}(x)$  is the exponential integral function. In order to extend (25) to trapped condensates, we replace the chemical potential within a local density approximation which includes the thermal atoms, i.e.

$$\mu \rightarrow g_{\text{q2D}}[n_c(r) + 2\tilde{n}(r)]. \quad (26)$$



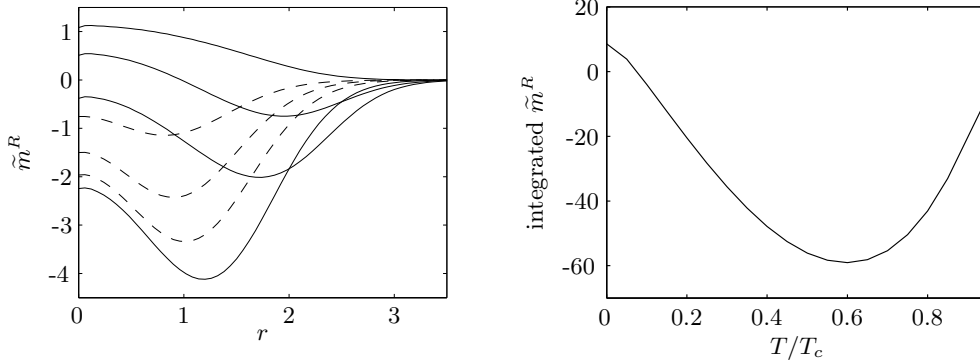


**Figure 1.** Renormalized anomalous average. **Left:**  $\tilde{m}^R$  at the temperatures  $T/T_c$ : 0, 0.15, 0.3, 0.75 (solid lines from top to bottom), 0.85, 0.9 and 0.975 (dashed lines from bottom to top). The renormalization makes  $\tilde{m}^R$  positive at low temperatures. **Right:** Spatially integrated anomalous average as a function of the non-interacting gas critical temperature. Note that interactions decrease the critical temperature slightly (Gies & Hutchinson 2004).

In the following section we will compare this result to the finite-temperature numerical results of HFB theory.

### 3. Numerical Results

We now present the results of our numerical calculation. We use the G2 formalism and the numerical methods are outlined in (Hutchinson et al. 2000, Gies & Hutchinson 2004). All quantities are shown in trap units, i. e. lengths are scaled by the radial harmonic oscillator length  $l_{\perp} = \sqrt{\hbar/m\omega_{\perp}}$  and energies by  $E_0 = \hbar\omega_{\perp}/2$ . We consider a sample of 2000 sodium atoms. The critical temperature of the non-interacting gas is approximately 33 nK.

#### 3.1. The anomalous average

In the left panel of Figure 1 the renormalized anomalous average  $\tilde{m}^R$  is plotted at various temperatures. Often  $\tilde{m}$  is renormalized by simply dropping the ‘1’ in the term  $2f_B + 1$  in (9), which is responsible for its divergence. Then the anomalous average is negative at all times. At zero temperature, however, this implies  $\tilde{m} \equiv 0$ , which makes the gapless HFB result for the many-body T-matrix useless. Utilizing the semi-classical approximation to perform a more careful renormalisation, the anomalous average becomes positive at low temperatures.

As the temperature is increased towards the critical temperature, the condensate becomes highly depleted and the anomalous average vanishes. This is shown in the right panel of Figure 1.

#### 3.2. Interaction strength at zero temperature

To avoid confusion, we again point out that we refer to the many-body T-matrix of section 2.2 as the *quasi-2D coupling parameter*. The many-body T-matrix obtained numerically from the G2 theory is referred to as the *gapless HFB many-body T-matrix*.

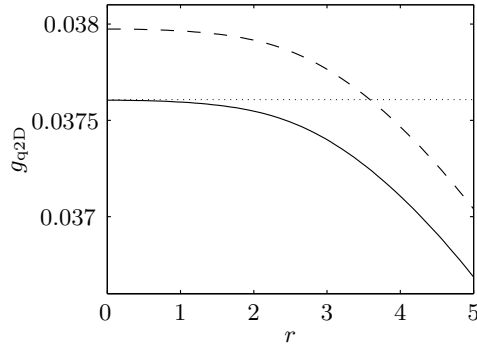


**Figure 2.** Quasi-2D coupling parameter at zero temperature. The full line corresponds to the spatially dependent, self-consistent solution of (23), the dashed line is the approximate solution (24). The dotted line is the homogeneous limit (21). The dimensional parameter is  $l_z/a_{3D} \approx 270$ . Note that the condensate density has dropped to below 1% of its peak value at a radius of  $3.5 l_{\perp}$  (Gies & Hutchinson 2004).

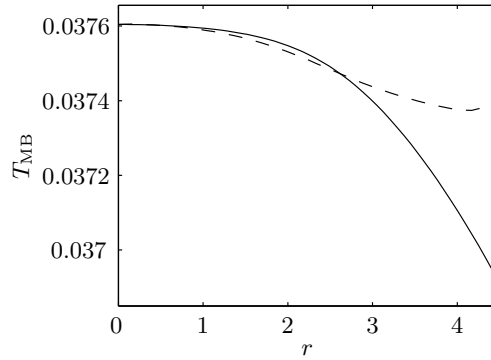


**Figure 3.** Comparison of the quasi-2D coupling parameter (solid line) and the gapless HFB many-body T-matrix (dashed line) at zero temperature. The gapless HFB result has been calculated with  $g$  chosen to achieve agreement in the trap centre. The parameter of confinement is  $l_z/a_{3D} \approx 270$ .

Figure 2 shows the quasi-2D coupling parameter for conditions corresponding to the recent MIT experiment (Görlitz et al. 2001), where  $l_z/a_{3D} \approx 270$ . In Figure 3 we compare the self-consistent result from the previous figure with the result from gapless HFB. The coupling strength  $g$  in (5) is chosen so that both versions of the many-body T-matrix agree in the trap centre. This leads to very good agreement between the two approaches in the region where interactions take place. At the edge of the condensate the gapless HFB many-body T-matrix returns to the value of  $g$ , which would be the two-body T-matrix in the three-dimensional case. The quasi-2D coupling parameter approaches zero in the case that  $n_c = 0$ , however it remains finite in the numerical calculation due to the weak logarithmic dependence on the condensate density.

Figure 4 is similar to Figure 3, but with the axial trapping frequency increased by a factor of  $10^4$ , corresponding to an axial length scale  $l_z/a_{3D} \approx 3$ , which pushes the condensate close to the genuine 2D limit. The agreement between the quasi-2D coupling parameter and the gapless HFB many-body T-matrix improves the more

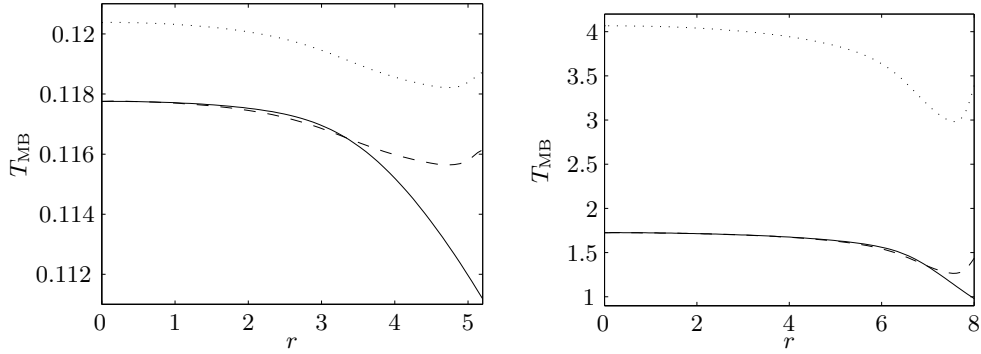


**Figure 4.** Comparison of the off-shell two-body many-body T-matrix (solid line) and the gapless HFB many-body T-matrix at zero temperature for different axial trapping frequencies. The dotted line corresponds to the choice of  $U_0 = g'_{3\text{D}}$ , the dashed line to  $U_0 = g_{\text{q2D}}^{\text{hom}}$ . With increasing trapping frequency, the condensate approaches the purely two-dimensional regime. In comparison to Figure 3, the ratio  $l_z/a_{3\text{D}}$  is decreased to 84 (left) and 3 (right). This corresponds to trapping frequencies of  $10^1$  and  $10^4$  times the original frequency of  $\omega_z = 2\pi 790$  Hz. The ordinate in all plots has been scaled to match the extension of the condensate, i. e. the radius of the condensate increases with increasing  $\omega_z$ .

‘two-dimensional’ the system becomes. Also shown is the gapless HFB many-body T-matrix where we have used  $g = g_{\text{q3D}}$  (dotted line). The smaller the parameter  $l_z/a_{3\text{D}}$ , the larger the gap between the results calculated using the quasi-2D and quasi-3D coupling parameters, indicating that the quasi-3D parameter, which considers scattering to take place in three dimensions, loses validity in this regime.

### 3.3. Results at finite temperatures

Finite temperature results for the many-body T-matrix, calculated within the gapless HFB formalism, are depicted in Figure 5. The parameter  $g$  in (5) does not depend on temperature, but only on the trap geometry, since finite temperature contributions are naturally incorporated through the anomalous average and the condensate density. Thus, we can determine  $g$  at zero temperature from comparison with the off-shell two-body T-matrix and use this parameter in the finite temperature calculations. This method relies on the agreement of the quasi-2D coupling parameter and the gapless HFB many-body T-matrix at zero temperature. In the previous section we have shown that these do agree in the quasi-2D limit in the spatial regime where condensate interactions take place. Comparable results for the gapless HFB many-body T-matrix have also been obtained for the three dimensional case (Hutchinson et al. 2000).

As can be seen in Figure 5, with increasing temperature and non-condensate fraction many-body effects cause the interaction strength to drop down to about 70% of its maximal value within the extent of the condensate.

The approximation of the many-body T-matrix via the off-shell two-body T-matrix in the zero-temperature limit cannot represent the behaviour of the gapless HFB result, even if the population term in (25) is included. In Figure 6 we explicitly show the discrepancy of the zero temperature quasi-2D coupling parameter (solid line) and the finite temperature gapless HFB many-body T-matrix (dashed line). If, however, we use the local density approximation (26) to replace the chemical potential

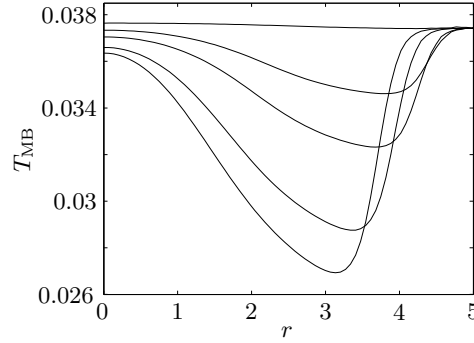


**Figure 5.** Gapless HFB many-body T-matrix at 0, 0.3, 0.5, 0.75 and 0.85  $T/T_c$  from top to bottom.

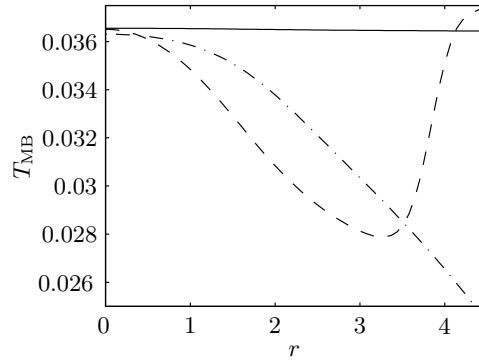


**Figure 6.** Many-body T-matrix at  $0.85 T_c$ : The solid line is the quasi-2D coupling parameter from Figure 3. The dashed line is the gapless HFB many-body T-matrix from Figure 5 with  $g$  determined at zero temperature as described in the text. The chained line corresponds to the solution of the finite temperature extension (25) within the local density approximation.

by the density term from the GPE, we get much better agreement even at temperatures as high as  $0.85 T_c$  (chained line).

Still, the result based on the approach in (Rajagopal et al. 2004) seems to underestimate finite-temperature many-body effects. We pointed out in Section 2.2.3 how problems occur in two dimensions when deriving the T-matrix from the homogeneous case. The major contribution to scattering effects comes from the highly occupied low-energy states. The finite-temperature effects on these low-lying states are not properly accounted for in the derivation of (25) from the homogeneous gas. Due to the large population the Bose-enhancement amplifies the effect of these states, and this is the reason for the discrepancy between the two approaches.

#### 4. Discussion

The determination of the many-body T-matrix is important in lower dimensional systems where scattering processes cannot be described merely by the two-body T-matrix. The effects of the surrounding many-body medium on condensate interactions must be taken into consideration at all temperatures.

In this paper we have presented results based on a gapless extension of the full HFB theory, used previously in the three dimensional case (Hutchinson *et al.* 2000). The self-consistent HFB method allows the determination of the many-body T-matrix for the whole temperature regime below the critical temperature. Approaches complementary to the HFB method exist, and we compare our results to a quasi-two-dimensional coupling parameter obtained from evaluating the off-shell two-body T-matrix in two dimensions. Lee *et al* have shown that this corresponds to the many-body T-matrix if evaluated at a shifted collision energy (Lee *et al.* 2002). We find that the gapless HFB many-body T-matrix agrees well with the results obtained from the off-shell two-body T-matrix at zero temperature. Depending on the strength of the axial confining potential, the agreement improves as the system changes from close to the quasi-3D to the quasi-2D regime, as this is the relevant regime for the calculation. The agreement between the two different approaches confirms the validity of the semi-classical renormalization method we employ to remove the ultra-violet divergence of the anomalous average.

On close examination of the finite temperature results, we see that the many-body T-matrix develops a strong spatial dependence, decreasing in strength towards the edge of the condensate. While finite temperature contributions to many-body effects on scattering are neglected in the approximation used in (Lee *et al.* 2002), an extension to finite temperatures has recently been presented for the homogeneous case by Rajagopal *et al* (Rajagopal *et al.* 2004). The inclusion of a population factor due to the Bose distribution in (18) leads to a decrease in the homogeneous interaction strength with increasing temperature, which we confirm. However, the previously mentioned spatially dependent decrease is much more dominant than this shift. By invoking a local density approach, we obtain much better agreement between the gapless HFB many-body T-matrix and the finite temperature version of the quasi-2D coupling parameter even at high temperatures, although the latter underestimates finite-temperature many-body effects on scattering. The reason for this we identify as an inappropriate treatment of the strongly contributing low-energy states, originating in the derivation of the coupling parameter for the homogeneous gas. The phonon modes which have been neglected in the treatment of Rajagopal *et al* appear to be significant. These modes are included in the G2 numerical results.

The self-consistent gapless HFB calculation requires the choice of a temperature independent two-body coupling strength to start with. Having shown that the gapless HFB and the off-shell two-body T-matrix approach agree very well at zero temperature, we can determine this parameter by matching the gapless HFB result to the quasi-2D coupling parameter. The parameter depends only on the trap geometry and can, therefore, be used for the finite temperature calculation where the result from (Lee *et al.* 2002) is no longer valid. Our approach therefore renders a consistent technique which is easy to implement and valid for all temperatures below the transition temperature.

In conclusion, we have shown that the many-body T-matrices determined from two very different approaches, the gapless HFB theory with a semi-classically renormalized anomalous average and the off-shell two-body T-matrix, agree very well at zero temperature and throughout a large spatial regime at finite temperatures.

## Acknowledgments

We would like to acknowledge the Marsden Fund of the Royal Society of New Zealand and the Royal Society (London) for financial support. We would also like to thank Sam Morgan for exceedingly useful discussions.

## References

- Bijlsma M J & Stoof H T C 1997 *Phys. Rev. A* **55**(1), 498.  
Fischer D S & Hohenberg P C 1988 *Phys. Rev. B* **37**(10), 4936.  
Gies C & Hutchinson D A W 2004 *preprint cond-mat/0406210*.  
Gies C, van Zyl B P, Morgan S A & Hutchinson D A W 2004 *Phys. Rev. A* **69**(2), 023616.  
Goldstone J 1961 *Nuovo Cimento* **19**, 154.  
Görlitz A, Vogels J M, Leanhardt A E, Raman C, Gustavson T L, Abo-Shaeer J R, Chikkatur A P, Gupta S, Inoué S, Rosenband T & Ketterle W 2001 *Phys. Lett.* **87**(13), 130402.  
Griffin A 1996 *Phys. Rev. B* **53**(14), 9341.  
Huang K 1987 *Statistical Mechanics* 2nd edn John Wiley & Sons, New York.  
Hugenholtz N M & Pines D 1959 *Phys. Rev.* **116**(3), 489.  
Hutchinson D A W, Burnett K, Dodd R J, Morgan S A, Rusch M, Zaremba E, Proukakis N P, Edwards M & Clark C W 2000 *J. Phys. B* **33**, 3825.  
Hutchinson D A W, Dodd R J & Burnett K 1998 *Phys. Rev. Lett.* **81**(11), 2198.  
Hutchinson D A W & Morgan S A 2002 *Laser Phys.* **12**(1), 84.  
Hutchinson D A W, Zaremba E & Griffin A 1997 *Phys. Rev. Lett.* **78**(10), 1842.  
Khawaja U A, Andersen J O, Proukakis N P & Stoof H T C 2002 *Phys. Rev. A* **66**, 013615.  
Kolomeisky E B, Newman T J, Straley J P & Qi X 2000 *Phys. Rev. Lett.* **85**(6), 1146.  
Kolomeisky E B & Straley J P 1992 *Phys. Rev. B* **46**(18), 11749.  
Lee M D, Morgan S A, Davis M J & Burnett K 2002 *Phys. Rev. A* **65**, 043617.  
Morgan S A 2000 *J. Phys. B* **33**, 3847.  
Morgan S A, Lee M D & Burnett K 2002 *Phys. Rev. A* **65**(2), 0220706.  
Petrov D S, Holzmann M & Shlyapnikov G V 2000 *Phys. Rev. Lett.* **84**(12), 2551.  
Petrov D S & Shlyapnikov G V 2001 *Phys. Rev. A* **64**, 012706.  
Proukakis N P, Morgan S A, Choi S & Burnett K 1998 *Phys. Rev. A* **58**(3), 2435.  
Rajagopal K K, Vignolo P & Tosi M P 2004 *Physica B – Condensed Matter* **344**, 157.  
Reidl J, Csordás A, Graham R & Szépfalussy P 1999 *Phys. Rev. A* **59**(5), 3816.  
Schick M 1971 *Phys. Rev. A* **3**, 1067.  
Stoof H T C & Bijlsma M 1993 *Phys. Rev. E* **47**(2), 939.  
Stoof H T C, de Goey L P H, Rovers W M H M, Jansen P S M K & Verhaar B J 1988 *Phys. Rev. A* **38**(3), 1248.  
Tanatar B, Minguzzi A, Vignolo P & Tosi M P 2002 *Physics Letters A* **302**, 131.